

Catalytic Reduction of Hydrazine to Ammonia by a Mononuclear Iron(II) Complex on a Tris(thiolato)phosphine Platform

Ya-Ho Chang,[†] Pooi-Mun Chan,[†] Yi-Fang Tsai,[†] Gene-Hsiang Lee,[‡] and Hua-Fen Hsu^{*,†}[†]Department of Chemistry, National Cheng Kung University, Tainan 701, Taiwan[‡]Department of Chemistry, National Taiwan University, Taipei 106, Taiwan

S Supporting Information

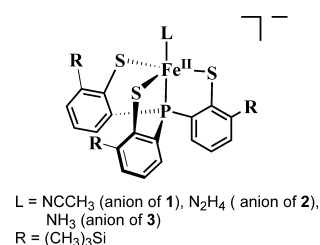
ABSTRACT: To provide the mechanistic information of nitrogenase at a molecular level, much effort has been made to develop synthetic metal complexes that have enzyme-like reactivity. Herein we obtain an iron(II) complex binding with a tris(thiolato)phosphine ligand, $[\text{P}(\text{Ph})_4][\text{Fe}(\text{PS}3'')(\text{CH}_3\text{CN})]$ (**1**; $\text{PS}3'' = \text{P}(\text{C}_6\text{H}_3\text{-}3\text{-Me}_3\text{Si-}2\text{-S})_3^{3-}$) that catalyzes the reduction of hydrazine, an intermediate and a substrate of nitrogenase. The substrate- and product-bound adducts, $[\text{N}(\text{Bu})_4][\text{Fe}(\text{PS}3'')(\text{N}_2\text{H}_4)]$ (**2**) and $[\text{N}(\text{Et})_4][\text{Fe}(\text{PS}3'')(\text{NH}_3)]$ (**3**), respectively, are also synthesized. This work provides the feasibility that the late stage of biological nitrogen fixation can be conducted at a single iron site with a sulfur-rich ligation environment.

Development of synthetic metal complexes that activate small molecules relevant to nitrogenous substrates continues to grow.¹ This endeavor strives to elucidate the mechanism of biological nitrogen fixation carried out by nitrogenases as well as the Haber-Bosch process.² Despite the finely described structural information given by a molybdenum-dependent enzyme,³ the detailed steps for substrate binding and activation remain relatively undefined.⁴ A combined biochemical–genetic investigative strategy revealed intermediates in the catalytic cycle having been trapped and identified as N_2H_2 - and N_2H_4 -bound FeMo cofactors through ENDOR/ESEEM spectroscopies; these are associated with the middle and late stages of nitrogen fixation, respectively.⁵ Furthermore, studies also suggest that waisted iron ion(s) in the FeMo cofactor near essential amino acids (α -70-Val and α -195-His) might be a catalytic pocket.⁶

On the basis of these studies, much work has been devoted to the synthesis of metal complexes that conduct nitrogenous transformation.⁷ N_2H_4 has been identified as a substrate and an intermediate of the enzyme.⁸ Unfortunately, reported synthetic analogues that catalyze the reduction of hydrazine to ammonia, mimicking the late stage of nitrogen fixation, are very limited.⁹ They are mostly early-transition-metal complexes including molybdenum, tungsten, and vanadium cases. Only two diiron complexes, obtained by Qu et al. and Nishibayashi et al., show the catalytic reactivity of hydrazine reduction.^{9h,i} In addition, an iron(II) complex with a pincer-type bis(pyrazole)pyridine ligand was reported recently to catalyze disproportionation of hydrazine into ammonia and dinitrogen.¹⁰ In this work, we utilize a tris(thiolato)phosphine ligand, $\text{P}(\text{C}_6\text{H}_3\text{-}3\text{-Me}_3\text{Si-}2\text{-S})_3^{3-}$ ($\text{PS}3''$),¹¹ as a platform to obtain an iron(II) complex,

$[\text{P}(\text{Ph})_4][\text{Fe}(\text{PS}3'')(\text{CH}_3\text{CN})]$ (**1**; Chart 1). This complex was found to catalyze the reduction of hydrazine to ammonia.

Chart 1



Furthermore, the substrate- and product-bound adducts, $[\text{N}(\text{Bu})_4][\text{Fe}(\text{PS}3'')(\text{N}_2\text{H}_4)]$ (**2**) and $[\text{N}(\text{Et})_4][\text{Fe}(\text{PS}3'')(\text{NH}_3)]$ (**3**), respectively, were synthesized and characterized (Chart 1).

The reaction of $\text{Li}_3[\text{PS}3'']$ and FeCl_2 in acetonitrile generated an emerald solution. After $[\text{P}(\text{Ph})_4]\text{Br}$ and ether were added, the solution was placed at $-30\text{ }^\circ\text{C}$ for 3 days to yield a crystalline solid of 1·4MeCN·Et₂O. Complex **2** was obtained from a reaction mixture of $\text{Li}_3[\text{PS}3'']$ and FeCl_2 in ethanol followed by the addition of excess $\text{N}_2\text{H}_4\cdot\text{H}_2\text{O}$. After the addition of $[\text{N}(\text{Bu})_4]\text{Br}$, the reaction mixture was kept at $-15\text{ }^\circ\text{C}$ for 2 days to afford a green crystalline precipitate of 2·5EtOH. A reaction mixture of $\text{Li}_3[\text{PS}3'']$ and FeCl_2 in ethanol was charged with NH_3 gas (1 atm) to provide a green solution. After $[\text{N}(\text{Et})_4]\text{Br}$ was added, the solution was kept at $-15\text{ }^\circ\text{C}$. A green crystalline solid of 3·3EtOH was precipitated after 2 days.

The structures of **1–3** were determined by X-ray crystallography. All three complexes crystallized with solvent molecules: four MeCN and one Et₂O molecules for **1**; five EtOH molecules for **2**; three EtOH molecules for **3**. Notably, the solvent molecules formed tight hydrogen-bonding networks that nicely filled the voids in the structures of **2** and **3** (Figures S1 and S2 in the Supporting Information, SI). The structures of the three complexes all contain a five-coordinate iron(II) center with trigonal-bipyramidal geometry (τ values of **1–3** are 0.98, 0.97, and 0.99, respectively)¹² by binding to a $\text{PS}3''$ ligand and an additional nitrogen-donor ligand (Figure 1). Other $\text{PS}3''$ derivatives of iron(II) complexes with CO, CN^- , and NO coligands have been reported previously as hydrogenase model compounds.¹³ The average Fe–S bond distances of 2.279, 2.290, and 2.300 Å found in **1–3**, respectively, are comparable to those

Received: August 16, 2013

Published: December 30, 2013

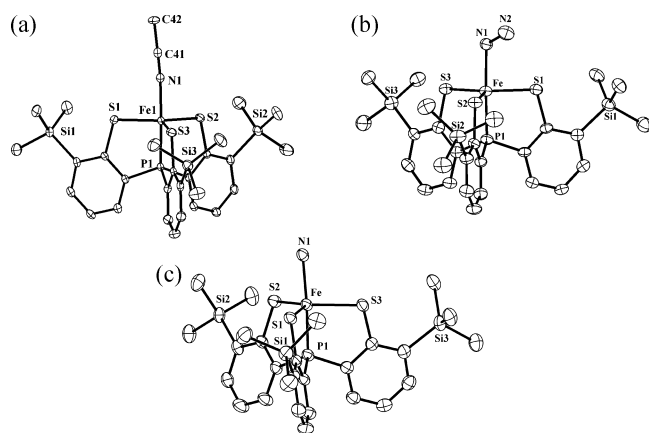


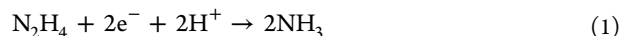
Figure 1. ORTEP diagrams of **1**·4MeCN·Et₂O (a), **2**·5EtOH (b), and **3**·3EtOH (c) shown with 35% thermal ellipsoids. The cations, solvent molecules, and hydrogen atoms are omitted for clarity. Selected bond lengths and angles are shown in Tables S1 and S2 in the SI.

found in iron(II) thiolate complexes (2.278–2.325 Å).¹³ The N–N bond distance of a bound hydrazine molecule in **2** is 1.451 Å, in agreement with those of existing iron(II) hydrazine complexes.¹⁴ The distances of N1···S1 (3.072 Å), N1···S2 (3.167 Å), and N1···S3 (3.169 Å) in **2** are within the range of hydrogen bonds, implying intramolecular hydrogen-bonding interactions between three thiolates and the bound hydrazine molecule (Figure S1 in the SI). Similarly, the structure of **3** also shows the same interaction between thiolate donors and a bound ammonia molecule based on the distances of ammonia and thiolates (N1···S1 = 3.149 Å, N1···S2 = 3.167 Å, and N1···S3 = 3.278 Å; Figure S2 in the SI). In addition, the ligated hydrazine molecule in **2** interacts with a crystallized solvent molecule, EtOH, through a hydrogen bond.

The magnetic measurement of **1** gave a μ value of 2.88 μ_B (Figure S3 in the SI), closed to the spin-only value (2.83 μ_B) for ground state $S = 1$, in agreement with a low-spin d^6 species in trigonal-bipyramidal geometry. The ¹H NMR spectrum taken in CD₃CN displays a characteristic peak at –10.45 ppm, consistently indicating that **1** is a paramagnetic species (Figure S4 in the SI). The electronic spectrum of **1** measured in MeCN exhibits two bands at 418 nm ($\epsilon = 5.13 \times 10^3 \text{ M}^{-1} \text{ cm}^{-1}$) and 602 nm ($\epsilon = 2.48 \times 10^3 \text{ M}^{-1} \text{ cm}^{-1}$) in the visible region, as well as a broad band in the near-IR region (Figure S5 in the SI). The cyclic voltammogram of **1** taken in MeCN shows two reversible oxidation waves at –0.813 V ($\Delta E = 99 \text{ mV}$) and 0.056 V ($\Delta E = 86 \text{ mV}$) versus Fc/Fc⁺, likely associated with Fe^{II/III} and Fe^{III/IV} redox couples, respectively (Figure S6 in the SI). The presence of a shoulder at –0.008 V might be indicative of a minor species from the decomposition of **1** at an Fe^{IV} oxidation state. The bound N₂H₄ and NH₃ molecules in **2** and **3**, respectively, are labile in both powder and solution forms. The nature of the lability at the apical site is essential for the catalytic system; however, it is a challenge for compound characterization. The N–H vibration of the bound hydrazine molecule in **2** can be located in IR spectroscopy, showing peaks at 3300, 3187, 3125, and 3081 cm^{–1}. The elemental analysis data of **2** and **3** both show a lower percentage of nitrogen atoms in the composition compared to the expected values. The electronic and ¹H NMR spectra of **2** and **3** taken in both acetonitrile and dimethyl sulfoxide resemble those of **1** (Figures S4 and S5 in the SI), indicating that axial coligands are easily replaced by donor solvent molecules. In the presence of excess N₂H₄, the electronic

spectrum of **2** displays the same absorption features (Figure S7 in the SI). However, the spectrum of **3** in an NH₃ atmosphere shows a difference of the relative intensity for two bands in the visible region (Figure S8 in the SI). The crystallographic data for **2** and **3** were successfully rendered because of the packed solvent molecules as well as inter- and intramolecular hydrogen-bonding interactions that assisted in stabilizing the bound hydrazine and ammonia, respectively.

The catalytic reactivity of **1** for the reduction of hydrazine was investigated in MeCN at ambient temperature and pressure with the addition of an external reductant and a proton source, [CoCp₂] and [LutH][BAR'₄] (CoCp₂ = cobaltocene, LutH = 2,6-lutidinium, and Ar' = 3,5-(CF₃)₂C₆H₃; eq 1), respectively.¹⁵



In a typical run, a mixture of complex **1** and 12 equiv of CoCp₂ was dissolved in MeCN followed by the addition of 6 equiv of N₂H₄ and 12 equiv of [LutH][BAR'₄]. At the end of the reaction time, the solution was quenched by HCl for product analysis. The results for the time-course studies are listed in Table S4 in the SI. The conversion of N₂H₄ to NH₃ reaches a maximum (~83%) at approximately 30 min. To ensure a nitrogen-atom balance, analyses for N₂H₄ were carried out for the reactions quenched at 30 min. Approximately 1 equiv of N₂H₄ (17%) was detected at the end of the reaction. For the control experiment, the same reaction was run in the absence of complex **1**, and less than 5% of the produced ammonia was detected. Hydrazine can be decomposed to ammonia and dinitrogen, as shown in eq 2. To estimate the amount of the ammonia produced from the pathway of disproportionation rather than reduction, the reactions were run without the addition of electron and proton sources. As shown in Table S3 in the SI, the detected ammonia only reaches 8% after 30 min and 15.6% in 1 h. Therefore, under the 60 min reaction time, the produced ammonia was mainly from the catalytic reduction of substrate. The reactions with various ratios of hydrazine to complex **1**, under the same conditions, were also studied. The results indicate that a maximum turnover number of 5–6 can be reached for the catalytic efficiency (Table 1).



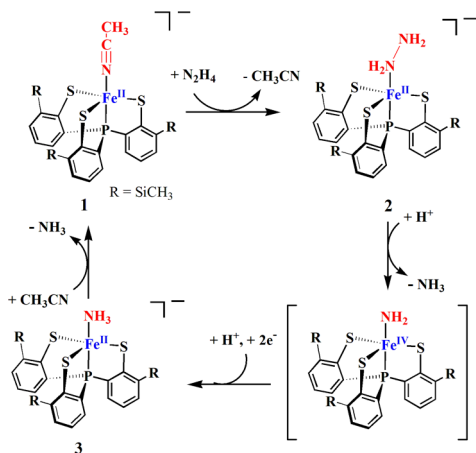
Table 1. Ammonia Production for the Catalytic Reduction of Hydrazine at Various Ratios of Hydrazine to **1**^a

added N ₂ H ₄ (equiv)	NH ₃ yield (mole)	NH ₃ yield (equiv)	conversion (%)	turnover
1.0	5.00×10^{-5}	2.0	100	1.0
2.0	1.00×10^{-4}	4.0	100	2.0
3.0	1.49×10^{-4}	5.9	99	3.0
5.0	2.25×10^{-4}	9.0	90	4.5
6.0	2.50×10^{-4}	10.0	83	5.0
10.0	2.77×10^{-4}	11.1	55	5.5

^a 2.50×10^{-5} mol of **1**, 2 equiv of Co(Cp)₂, and 2 equiv of [LutH][BAR'₄] (based on N₂H₄) were used for each reaction in MeCN. The reaction time was 30 min.

The independent isolation of substrate- and product-bound mononuclear iron(II) complexes, **2** and **3**, respectively, suggests that the catalytic reaction occurs at a single iron site supported by a PS3[–] ligand. The proposed pathway is shown in Scheme 1. The bound CH₃CN molecule in **1** is replaced by a N₂H₄ molecule to generate a substrate-bound adduct, **2**. Because **2** can be isolated in ethanol, the N–N bond of the bound hydrazine in the iron(II)

Scheme 1



center is not activated at this stage. Thus, protonation of the bound hydrazine from the addition of an external proton source is a key step for cleavage of the N–N bond. Subsequently, the first 1 equiv of ammonia is released and a corresponding Fe^{IV}NH₂ intermediate is likely generated. The access of an Fe^{IV} state supported by the PS3'' ligand system is demonstrated by the electrochemical data in this work, as well as isolation of an iron(IV) complex, [Fe(PS3'')Cl], reported by George et al.¹⁶ Finally, the second protonation with the presence of an external electron resource brings Fe^{IV}NH₂ to the Fe^{II}NH₃ state, followed by the release of a second 1 equiv of an NH₃ molecule. Our attempts to isolate the intermediates Fe^{II}N₂H₄, Fe^{IV}NH₂, and Fe^{II}NH₃ in MeCN used for catalysis were not successful. However, both Fe^{II}N₂H₄ and Fe^{II}NH₃ can be obtained in ethanol through stabilization of the hydrogen-bonding network in the crystalline form.

In summary, complex 1 serves as a catalyst for the reduction of hydrazine to ammonia, mimicking the late stage of biological nitrogen fixation. Notably, the iron center of 1 is in a sulfur-rich ligation environment, similar to those of the iron sites in the FeMo cofactor. Complex 1 represents the only example of a mononuclear iron thiolate complex that carries the reduction of hydrazine catalytically. While there are many controversial debates regarding the site of the substrate binding and activation in the FeMo cofactor, this work provides the likelihood that a single iron center in the FeMo cofactor can bind and activate an alternative substrate of nitrogenase, as well as play a role in the late stage of nitrogen fixation.

■ ASSOCIATED CONTENT

Supporting Information

Experimental details and crystallographic data in CIF format for 1–3. This material is available free of charge via the Internet at <http://pubs.acs.org>.

■ AUTHOR INFORMATION

Corresponding Author

*E-mail: konopka@mail.ncku.edu.tw.

Notes

The authors declare no competing financial interest.

■ ACKNOWLEDGMENTS

We thank the National Science Council in Taiwan (Grant NSC 99-2113-M-006-004-MY3) for financial support of this work.

■ REFERENCES

- (1) (a) Perters, J. C.; Mehn, M. P. In *Activation of small molecules*; Wiley-VCH: New York, 2006; p 81. (b) Hazari, N. *Chem. Soc. Rev.* **2010**, *39*, 4044–4056.
- (2) Scheibel, M. G.; Schneider, S. *Angew. Chem., Int. Ed.* **2012**, *51*, 4529.
- (3) (a) Einsle, O.; Tezcan, F. A.; Andrade, S. L. A.; Schmid, B.; Yoshida, M.; Howard, J. B.; Rees, D. C. *Science* **2002**, *297*, 1696–1700. (b) Spatzal, T.; Aksoyoglu, M.; Zhang, L.; Andrade, S. L. A.; Schleicher, E.; Weber, S.; Rees, D. C.; Einsle, O. *Science* **2011**, *334*, 940. (c) Lancaster, K. M.; Roemelt, M.; Ettenhuber, P.; Hu, Y.; Ribbe, M. W.; Neese, F.; Bergmann, U.; DeBeer, S. *Science* **2011**, *334*, 974–997.
- (4) (a) Schrock, R. R. *Angew. Chem., Int. Ed.* **2008**, *47*, 5512–5522. (b) Seefeldt, L. C.; Dance, I. G.; Dean, D. R. *Biochemistry* **2004**, *43*, 1401.
- (5) Hoffman, B. M.; Dean, D. R.; Seefeldt, L. C. *Acc. Chem. Res.* **2009**, *42*, 609–619.
- (6) Lukoyanov, D.; Dikanov, S. A.; Yang, Z.-Y.; Barney, B. M.; Samoilova, R. I.; Narasimhulu, K. V.; Dean, D. R.; Seefeldt, L. C.; Hoffman, B. M. *J. Am. Chem. Soc.* **2011**, *133*, 11655–11664.
- (7) (a) Yandulov, D. V.; Schrock, R. R. *Science* **2003**, *301*, 76–78. (b) Arasehira, K.; Miyake, Y.; Nishibayashi, Y. *Nat. Chem.* **2011**, *3*, 120–125. (c) Rodriguez, M. M.; Bill, E.; Brennessel, W. W.; Holland, P. L. *Science* **2011**, *334*, 780–783.
- (8) (a) Thorneley, R. N. F.; Eady, R. R.; Lowe, D. J. *Nature* **1978**, *272*, 557. (b) Barney, B. M.; Yang, T.-C.; Igarashi, R. Y.; Dos Santos, P. C.; Laryukhin, M.; Lee, H.-I.; Hoffman, B. M.; Dean, D. R.; Seefeldt, L. C. *J. Am. Chem. Soc.* **2005**, *127*, 14960–14961.
- (9) (a) Schrock, R. R.; Glassman, T. E.; Vale, M. G. *J. Am. Chem. Soc.* **1991**, *113*, 725–726. (b) Block, E.; Ofori-Okai, G.; Kang, H.; Zubieta, J. *J. Am. Chem. Soc.* **1992**, *114*, 758–759. (c) Schrock, R. R.; Glassman, T. E.; Vale, M. G.; Kol, M. *J. Am. Chem. Soc.* **1993**, *115*, 1760–1772. (d) Coucouvanis, D.; Mosier, P. E.; Demadis, K. D.; Patton, S.; Malinak, S. M.; Kim, C. G.; Tyson, M. A. *J. Am. Chem. Soc.* **1993**, *115*, 12193–12194. (e) Malinak, S. M.; Demadis, K. D.; Coucouvanis, D. *J. Am. Chem. Soc.* **1995**, *117*, 3126–3133. (f) Hitchcock, P. B.; Hughes, D. L.; Maguire, M. J.; Marjani, K.; Richards, R. L. *J. Chem. Soc., Dalton Trans.* **1997**, 4747–4752. (g) Chu, W.-C.; Wu, C.-C.; Hsu, H.-F. *Inorg. Chem.* **2006**, *45*, 3164–3166. (h) Chen, Y.; Zhou, Y.; Chen, P.; Tao, Y.; Li, Y.; Qu, J. *J. Am. Chem. Soc.* **2008**, *130*, 15250–15251. (i) Yuki, M.; Miyake, Y.; Nishibayashi, Y. *Organometallics* **2012**, *31*, 2953–2956.
- (10) Umehara, K.; Kuwata, S.; Ikariya, T. *J. Am. Chem. Soc.* **2013**, *135*, 6754–6757.
- (11) Block, E.; Ofori-Okai, G.; Zubieta, J. *J. Am. Chem. Soc.* **1989**, *111*, 2327.
- (12) Addison, A. W.; Rao, T. N.; Reedijk, J.; Vanrijn, J.; Verschoor, G. C. *J. Chem. Soc., Dalton Trans.* **1984**, 1349–1356.
- (13) (a) Nguyen, D. H.; Hsu, H.-F.; Millar, M.; Koch, S. A.; Achim, C.; Bominaar, E. L.; Münck, E. *J. Am. Chem. Soc.* **1996**, *118*, 8963–8964. (b) Hsu, H.-F.; Koch, S. A.; Popescu, C. V.; Münck, E. *J. Am. Chem. Soc.* **1997**, *119*, 8371–8372. (c) Conradie, J.; Quarless, D. A., Jr.; Hsu, H.-F.; Harrop, T. C.; Lippard, S. J.; Koch, S. A.; Ghosh, A. *J. Am. Chem. Soc.* **2007**, *129*, 10446–10456.
- (14) (a) Sellmann, D.; Soglowek, W.; Knoch, F.; Ritter, G.; Dengler, J. *Inorg. Chem.* **1992**, *31*, 3711–3717. (b) Sellmann, D.; Shaban, S.; Heinemann, F. *Eur. J. Inorg. Chem.* **2004**, *2004*, 4591–4601. (c) Crossland, J. L.; Zakharov, L. N.; Tyler, D. R. *Inorg. Chem.* **2007**, *46*, 10476–10478. (d) Field, L. D.; Li, H. L.; Dalgarno, S. J.; Turner, P. *Chem. Commun.* **2008**, 1680–1682. (e) Lee, Y.; Mankad, N. P.; Peters, J. C. *Nat. Chem.* **2010**, *2*, 558.
- (15) Reger, D. L.; Wright, T. D.; Little, C. A.; Lamba, J. J. S.; Smith, M. D. *Inorg. Chem.* **2001**, *40*, 3810–3814.
- (16) Niemoth-Anderson, J. D.; Clark, K. A.; George, T. A.; Ross, C. R. *J. Am. Chem. Soc.* **2000**, *122*, 3977–3978.

■ NOTE ADDED AFTER ASAP PUBLICATION

This paper was published on the Web on December 30, 2013, with errors in Figure 1. The corrected version was reposted on January 7, 2014.